

The statistical description and TOA placement feasibility analysis of ultra-wide band in-vehicle channel measurements

S MUNIRAJA¹, G. MANGA RAO²

Assistant professor^{1,2}

DEPARTMENT OF ELECTRICAL AND ELECTRONICS ENGINEERING
P.B.R.VISVODAYA INSTITUTE OF TECHNOLOGY & SCIENCE
S.P.S.R NELLORE DIST, A.P, INDIA, KAVALI-524201

Abstract

In-vehicle wireless channel measurements in the ultra-wideband (UWB) range of 3–11 GHz are reported here. The impacts of both the antenna's location and the presence of people in the vehicle's passenger compartment are investigated. Channel impulse responses (CIRs) have been computed by inverse Fourier transform from frequency domain data. The impact of picking a certain band group throughout the whole UWB spectrum is also detailed. In order to characterize the wireless channel statistics, a generalized extreme value procedure is used to the measured channel transfer functions. All possible combinations of antenna location and passenger occupancy are considered, and related parameter sets are calculated and recorded. We have also conducted a feasibility study of a TOA-based in-vehicle UWB localization system. Average error and standard deviation are used to assess the positioning accuracy.

Keywords:

Ultra-Wideband; Car Environment; Channel Model; Geolocation; Time-of-Arrival.

Introduction

Modern cars rely on cable bundles to implement their electrical power distribution, communication, and networking capabilities on the road. Sensors, actuators, control units, and information and entertainment systems seem to be proliferating in today's automobiles. The wiring in all cars becomes heavier as a direct consequence. The job of installing them in a way that is both flexible and reliable is difficult and expensive [1]. When cars are run entirely on electricity, the burden of the wiring only increases. In [2,3], the authors draw the inference that ultra-wide band with (UWB) technology, with its low transmit power and resilience against multipath fading, is suitable for use in the passenger compartment of vehicles. Authors in [4-9] and [3,10] tried to replace cable bundle start-up with in-vehicle radio channel measurements; [11,12] looked at a clustering technique for intra-bus channel modelling. Both the passenger and engine compartments of a car have seen attempts at prototyping a UWB-based wireless sensor network ([13,14]). Wireless LTE in-vehicle communication networks considering unique in-vehicle impulse noise are explored in [15]. The spatial stationarity of the UWB channel within a moving vehicle is investigated in [16]. Understanding the channel's specific characteristics is crucial for the efficient physical layer design of any wireless communication system. The need for a wireless localization service inside the vehicle goes hand in hand with the need to replace at least some of the car's cable bundles with wireless connectivity. In the future, services like this will be used for things like beam steering to provide high-speed Internet to vehicles and remote keyless entry and ignition. In [14,17], a UWB-based localization service is investigated, and it is shown that, in general, the time of arrival (TOA) approach is able to provide sufficient spatial resolution for a number of applications because of the high temporal resolution of UWB impulses. The TOA is most effective in LOS situations, but it may be utilized in non-LOS situations as well, although with certain limitations. For TOA-based ranging in a multipath environment, the direct ray that travels from the transmitter to the receiver is crucial. The TOA method is useful when the beam must pass through barriers, but their attenuation does not prevent the beam from being detected. It is important to remember that in the United States, for instance, the frequency range from 1.99 to 10.6 GHz is unrestricted for communications and wall-penetrating radars, allowing for the inspection of non-metallic materials [14,18]. As a result, it is assumed that positioning precision may be adequate even in the challenging in-vehicle environment with OLOS propagation.

Instrumentation set-up

The Dynamic Range and Bandwidth of Measurements

Figure 1 depicts the whole measurement setup technique. The complex CIRs (below introduced by (1)) are measured in the frequency domain for two different bands, 3 to 11 GHz (entire UWB band with a bandwidth of $B = 8$ GHz) and 3.3168 to 4.752 GHz (first band group with a bandwidth of $B = 1.58$ GHz), using a four-port vector network analyser Agilent Technologies E5071C (VNA; Agilent Technologies Inc., Santa Clara, CA,

USA) (Figure 2). Figure 3 depicts the location of the car's RX and TX antennas inside the structure of the vehicle. More than 90 dB of dynamic range may be achieved in the measuring environment (PoutVNA = 5 dBm, IF bandwidth = 100 Hz). In the case of the full UWB band, the selected frequency step of 10 MHz yields 801 frequency points, while in the case of the first band group, the selected frequency step yields 159 frequency points. Phase stable coaxial cables were employed and included into the callibration procedure to prevent the observed phase accuracy from degrading owing to movements of the RX antenna. The Skoda Octavia 1.8 TSI is used for the test drive.

Positioning of Antennas

As shown in Figure 3, the TX antennae are installed on the left and right sides of the dashboard, the top corners of the windshield, and the rear section of the ceiling, while the RX antennas are installed in various positions within the automobile compartment (on all seats and in the boot). The channels are tested in both line-of-sight and non-line-of-sight conditions. Seat backs, dashboards, and passengers all contribute to poor line-of-sight (NLOS).

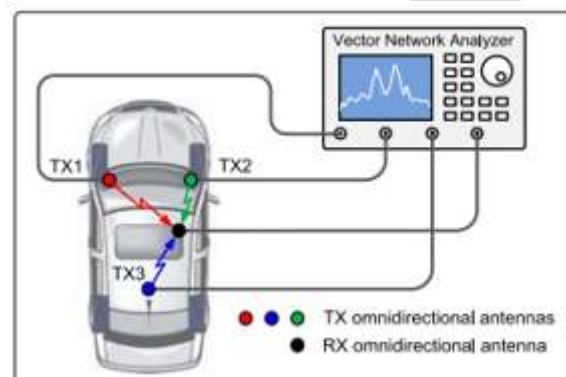


Figure 1 Measurement setup containing the vector network analyser Agilent Technologies E5071C and the car Skoda Octavia 1.8 TSI.



Figure 2 Images of the conical monopole antenna, measurement position, and four-port VNA. [left] Detail of the conical monopole antenna mounted on the front windshield. [middle] One measurement position inside the vehicle. [right] Four-port VNA connected with antennas inside the measured vehicle.

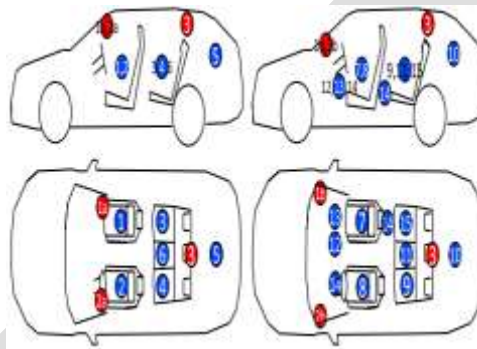
Because the conical monopole antenna's [20] radiation pattern is so similar to that of an omnidirectional antenna, we were able to pick up as many multipath components (reflected waves) as possible. The conical monopole's H-plane radiation pattern is shown in Figure 4 to be uniform over the frequency range of interest. The antennas were installed in the automobile compartment to take advantage of the almost constant top half E-plane radiation pattern rather than the variable gain in the bottom half (elevation angle from 90 degrees to minus 90 degrees). This indicates that the antenna was installed upside-down on the cabin ceiling. Thus, the LOS and NLOS are little impacted by the radiation pattern; however, the lower elevation angle may be affected by the non-ideal radiation pattern of the antennas due to the reflected waves coming from the TX antenna or impinge on the RX antenna.

Parameters of the channel

The CIR defines the range of the wireless connection. The sequence of windowed scattering parameters is transformed backwards using an inverse discrete Fourier transform, as shown below.

$$h^{\alpha}(n) = \sum_{k=0}^{N-1} w(k) s_{\zeta}^{\alpha}(k) e^{jkn2\pi/N},$$

where $s_{\alpha} \zeta(k)$ corresponds to the k th measured scattering parameter (as described in Section 2) and $w(k)$ represents the Blackman window. Parameter α denotes the spatial positions of the transmit and the receive antenna in the measured vehicle and $\zeta \in \{41, 42, 43\}$. For practicality in the following statistical processing, we arbitrarily merge indices α and ζ into one measurement number $a \in \{1, \dots, 90\}$. Hence, in the following, it is not possible to assign the specific measured data to the actual spatial positions.



The red and blue antennas in Figure 3 represent the transmission and reception locations, respectively. We use both the standard and the unconventional layout for the receiving antenna. The antennae 1a and 2a can be seen in the upper left and right corners of the windscreen, while the antennae 1b and 2b can be seen in the bottom left and right corners, respectively. Please be aware that all dimensions have been calculated considering a variety of passenger configurations. Two scenarios, one with no passengers and the other with two or three, have been studied.

Localization

Precise range and localization using the TOA technique is one of the most talked-about uses for UWB. This is due to the high temporal resolution (see Equation 7) and MPC separation made possible by the wide UWB bandwidth. We sought to get some understanding of the achievable range precision by measuring the channel transfer function for a wide variety of antenna placements. The complex inverse transfer function (CIR) provides the basis for our distance estimate. When compared to direct channel sounding in the time domain, where more sophisticated approaches like matched filtering of the known Gaussian pulses or a well-correlated binary sequence may be utilized, this method has its drawbacks [24]. We used the Time-of-Arrival (TOA) method to determine antenna distance from first ray detection.

Table 1 Summarization of GEV type I parameters characterizing in-vehicle environment for 90 permutations of antenna placement and car seat occupancy

	μ	σ	k
Distribution type	Lognormal	Normal	Logistic
Mean ν	48.37	5.48	-0.08
Variance η	31.05	0.26	0.002

from a particular antenna. The proposed threshold-based search algorithm compares individual signal samples of the CIR with a certain threshold in order to identify the amplitude peak corresponding to the first MPC. This approach allows to calculate distance also in the NLOS scenario because the first ray may not be the strongest ray. However, penetration of the obstacles can cause some measurement accuracy degradation (see below). The aim of this chapter is to give a basic idea about accessible average error and standard deviation of the measured

distances for the entire UWB band and for the first band group and also for the empty and occupied car. For more information about the measurements and the distance calculation, see [25]. Because all the particular measurements were done for three TX antennas and one RX antenna, we also calculated RX antenna position using the 2D localization technique in order to assess whether it corresponds at least roughly to reality, i.e., whether it is possible for example to reliably detect a device on a particular seat. Note that most of the above-mentioned application does not need an accurate localization but only rough estimation of the device position.

Basic system parameter calculation

The frequency band B determines the time resolution of measurement by [24]:

$$T_r = \frac{1}{B} = \frac{1}{F_U - F_L},$$

where F_U is the upper frequency and F_L is the lower frequency of the band. The propagation distance resolution is then

$$D_r = T_r c,$$

where $c = 2.998 \times 10^8$ m/s is the speed of the light. The maximum measurable propagation distance depends on the number of measured frequency values N_M inside the frequency band, i.e., on the frequency step f_s according to

$$D_{\max} = \frac{c}{B} N_M = \frac{c}{f_s}.$$

The preceding equations make it clear that decreasing the bandwidth and the number of frequency points used to calculate the propagation distance both reduce the distance resolution and the propagation distance that can be measured.

Conclusions

We conducted a large-scale UWB measuring experiment inside passenger vehicles. The GEV distribution is used to simulate the observed impulse responses of channels, and its parameters are computed by an MLE. Thus, the empirical measurement findings are almost in perfect agreement with our statistical description of the received amplitude and phase distribution in the in-vehicle environment. We demonstrated that the observed phase follows a iid distribution. An in-vehicle UWB positioning feasibility study was performed using the collected data. We demonstrated that, over the entire UWB bandwidth, a standard deviation of less than 10 cm was achievable in transmitter location accuracy. Only in the first UWB band group was the standard deviation less than 16 cm. The number of people in the automobile had a greater impact on localization precision than did the location of the antenna.

References

- [1]. G Leen, D Heffernan, *Expanding automotive electronic systems*. *Computer*. 35(1), 88–93 (2002)
- [2]. M Win, R Scholtz, *Characterization of ultra-wide bandwidth wireless indoor channels: a communication-theoretic view*. *Selected Areas Commun. IEEE J.* 20(9), 1613–1627 (2002)
- [3]. R-M Cramer, R Scholtz, M Win, *Evaluation of an ultra-wide-band propagation channel*. *Antennas Propag. IEEE Trans.* 50(5), 561–570 (2002)
- [4]. M Schack, J Jemai, R Piesiewicz, R Geise, I Schmidt, T Kurner, in *IEEE Vehicular Technology Conference, 2008. Measurements and analysis of an in-car UWB channel (VTC Spring 2008 Singapore, 11–14 May 2008)*, pp. 459–463
- [5]. T Kobayashi, in *2006 IEEE Ninth International Symposium on Spread Spectrum Techniques and Applications, Manaus-Amazon. Measurements and characterization of ultra wideband propagation channels in a passenger-car compartment*, (28–31 Aug 2006), pp. 228–232
- [6]. T Tsuboi, J Yamada, N Yamauchi, in *7th International Conference on ITS Telecommunications, 2007. ITST '07. UWB radio propagation inside vehicle environments (Sophia Antipolis, 6–8 June 2007)*, pp. 1–5

- [7]. M Schack, R Geise, I Schmidt, R Piesiewicz, T Kurner, in *3rd European Conference on Antennas and Propagation, 2009. EuCAP 2009. UWB channel measurements inside different car types (Berlin, 23–27 March 2009)*, pp. 640–644
- [8]. A Moghimi, H-M Tsai, C Saraydar, O Tonguz, *Characterizing intra-car wireless channels. Vehic. Technol. IEEE Trans.* 58(9), 5299–5305 (2009)
- [9]. J Blumenstein, T Mikulasek, R Marsalek, A Prokes, T Zemen, C Mecklenbrauker, in *2014 IEEE 80th Vehicular Technology Conference (VTC Fall). In-vehicle mm-wave channel model and measurement (Vancouver, BC, 14–17 Sept 2014)*, pp. 1–5
- [10]. PC Richardson, W Xiang, W Stark, *Modeling of ultra-wideband channels within vehicles. Selected Areas Commun. IEEE J.* 24(4), 906–912 (2006)
- [11]. L Liu, Y Wang, N Zhang, Y Zhang, in *2010 12th IEEE International Conference on Communication Technology (ICCT). UWB channel measurement and modeling for the intra-vehicle environments (Nanjing, 11–14 Nov 2010)*, pp. 381–384
- [12]. B Li, Z Zhou, D Li, S Zhai, *Efficient cluster identification for measured ultra-wideband channel impulse response in vehicle cabin. Prog. Electromagnetics Res.* 117, 121–147 (2011)
- [13]. J Li, T Talty, in *Military Communications Conference, 2006. MILCOM 2006. Channel characterization for ultra-wideband intra-vehicle sensor networks (Washington, DC, 23–25 Oct 2006)*, pp. 1–5
- [14]. R Thoma, O Hirsch, J Sachs, R Zetik, in *The Second European Conference on Antennas and Propagation, 2007. EuCAP 2007. UWB sensor networks for position location and imaging of objects and environments (Edinburgh, 11–16 Nov 2007)*, pp. 1–9
- [15]. J Blumenstein, R Marsalek, A Prokes, C Mecklenbrauker, in *Multiple Access Communications. Impulse noise mitigation for OFDM by time-frequency spreading*, vol. 8310 (ser. *Lecture Notes in Computer Science*. Springer International Publishing Vilnius, Lithuania, 16–17 Dec 2013), pp. 8–20
- [16]. J Blumenstein, T Mikulasek, R Marsalek, A Chandra, A Prokes, T Zemen, C Mecklenbrauker, in *IEEE Vehicular Networking Conference (VNC). In-vehicle UWB channel measurement, model and spatial stationarity (Paderborn, 3–5 Dec 2014)*, pp. 77–80
- [17]. R Fontana, E Richley, J Barney, in *2003 IEEE Conference on Ultra Wideband Systems and Technologies. Commercialization of an ultra wideband precision asset location system (Reston, VA, USA, 16–19 Nov 2003)*, pp. 369–373
- [18]. R-R Lao, J-H Tarn, C Hsiao, in *The 57th IEEE Semiannual Vehicular Technology Conference, 2003. VTC 2003-Spring. Transmission coefficients measurement of building materials for UWB systems in 3-10 GHz*, vol. 1 (Jeju, Korea, 22–25 April 2003), pp. 11–14
- [19]. Q Liang, A Audu, H Khani, H Nie, W Xiang, Z Chen, in *2013 IEEE Radio and Wireless Symposium (RWS). Measurement and analysis of intra-vehicle UWB channels (Austin, TX, USA, 20–23 Jan 2013)*, pp. 166–168
- [20]. JD Kraus, McGraw-Hill Education, (New York, 1988)
- [21]. RA Fisher, in *Mathematical Proceedings of the Cambridge Philosophical Society. Theory of Statistical Estimation*, (1925), pp. 700–725.